Comparison of Fast Measurement Methods for Short-Term Negative Bias Temperature Stress and Relaxation

Ph. Hehenberger*, P.-J. Wagner•, H. Reisinger°, and T. Grasser•
* Institute for Microelectronics, TU Wien, A-1040 Wien, Austria
• Christian Doppler Laboratory for TCAD at the Institute for Microelectronics, TU Wien, A-1040 Wien, Austria
° Infineon Technologies, D-81739 München, Germany

***Abstract*— The initial degradation during negative bias stress is often assumed to be due to hole trapping, while the generation of interface states may dominate at longer stress times. We conduct a thorough study of short-time negative bias temperature stress and relaxation using ultra-fast measurement techniques in the micro-seconds regime to clarify the physical mechanisms behind the responsible hole trapping phenomenon. We observe that the extracted degradation of the drain-current ΔI_{D} or the threshold-voltage ΔV_{TH} can be well fitted by a logarithmic time dependence. Only for stronger stresses, that is, higher temperatures and/or voltages, the data shows a detectable deviation from the logarithmic behavior, allowing for a power-law fit. The exponent of this power-law is about 0.04 and thus considerably smaller than the typically reported long-term exponents of about 0.12 to 0.15. We finally observe a strong field- and temperature-dependence of the initial degradation, which is incompatible with the frequently assumed elastic hole trapping mechanism but favors a thermally activated hole trapping process.**

Introduction

Shrinking device sizes and the requirements to operate at higher temperatures in up-to-date applications of MOS transistors result in accelerated degradation of crucial device parameters like the threshold voltage V_{TH} and the mobility. Of particular importance is the negative bias temperature instability (NBTI) [1, 2] which is observed when a negative bias is applied to the gate of pMOS transistors with the other contacts grounded. NBTI is considerably enhanced by temperature but the degradation shows similar features also at room temperature.

The initial degradation is commonly interpreted assuming elastic hole trapping due to tunneling carrier exchange with the substrate [1, 3]. Long-term degradation, on the other hand, is often assumed to be due to the creation of interface states [4, 5]. From an experimental point, elastic tunneling is usually identified as a roughly temperature-independent process following a logarithmic time dependence and experimental evidence for some thermally nitrided oxides has been given [6]. In contrast, long-term degradation is frequently reported to follow a power-law with exponents in the order of 0.12 to 0.15.

Previous experiments using conventional parameter analyzers with a time resolution in the milli-second regime indicate that at least for up to medium stresses, a logarithmic time dependence is observed during the first three decades ($1\,\mathrm{ms}$ up to $1\,\mathrm{s}$) [7]. This logarithmic short-term degradation shows a strong temperature activation similar to the long-term degradation ($E_{\mathrm{A}} \approx 0.1\,\mathrm{eV}$) and a super-linear stress field dependence ($\sim E_{\mathrm{ox}}^2$). For longer stress times and higher stress fields, degradation starts to deviate from the logarithmic behavior [7, 8].

In the following we will extend on our previous results [7, 9] and study short-term degradation using two different ultra-fast measurement techniques operating in the micro-second regime. By this measure we double the number of available decades from three to six during short-time stresses up to $1\,\mathrm{s}$. We furthermore compare recovery data obtained by two different ultra-fast techniques.

I. Fast Measurement Methods

Three fast measurement methods are commonly used for NBTI assessment [10]. *(i)* The on-the-fly (OTF) method [1, 11, 12] records the degradation during stress and hence does not introduce unwanted recovery, but suffers from the mobility degradation, which leads to a spurious ΔV_{TH} [13, 14]. *(ii)* The fast-V_{TH} method [15] briefly interrupts the stress (μs delay) to quickly record V_{TH} during recovery. *(iii)* The fast-I_{D} method [7, 16–19] works similarly to the fast-V_{TH} method but instead records the drain current $I_{\mathrm{D}}(V_{\mathrm{G}} \approx V_{\mathrm{TH}})$, which is then converted to ΔV_{TH} [7] using an initial $I_{\mathrm{D}}(V_{\mathrm{G}})$ curve. The OTF method as usually implemented on a parameter analyzer suffers from the problem that the initial reference current is obtained only after a pre-stress period of the length of the measurement delay. In contrast, the fast-V_{TH} and the fast-I_{D} methods can record an unstressed reference value but suffer from the delay during measurement [10, 16]. In the following we use the fast ramp method originally developed by Kerber with the improvements suggested in [10] for our short-term NBTI measurements in the range of $1\,\mu\mathrm{s}$ to $1\,\mathrm{s}$ [9] and compare the results against the fast-V_{TH} method of [15].

II. Samples Used and Stress Conditions

To perform the short-term NBTI degradation [9, 10], PMOSFETS from a standard $90\,\mathrm{nm}$ CMOS process with plasma-nitrided oxide (around $6\,\%$ of nitrogen) were used. A thin oxide device ($t_{\mathrm{ox}} = 1.8\,\mathrm{nm}$) with geometry $W/L = 10\,\mu\mathrm{m}/0.12\,\mu\mathrm{m}$ was used. The devices were stressed with gate voltages $V_{\mathrm{G,str}}$ of $-1.75\,\mathrm{V}$, $-2.00\,\mathrm{V}$, $-2.25\,\mathrm{V}$, and $-2.50\,\mathrm{V}$ at temperatures of $25\,^{\circ}\mathrm{C}$, $75\,^{\circ}\mathrm{C}$, $125\,^{\circ}\mathrm{C}$, and $175\,^{\circ}\mathrm{C}$.

III. Measurement Equipment and Setup

Typically, ultra-fast measurements in the micro-second regime suffer from noise. Since the amplitude resolution can be enhanced by averaging, while there is no remedy for a too slow measurement, we use a digital storage oscilloscope (DSO) to record multiple NBTI processes and take an average of these. Care has to be taken to conform to the preconditions of proper averaging, namely to record the *same* process many times to reduce the noise. In our measurements this is ensured by very short stress times and a very low duty cycle in order to achieve full relaxation between stresses. The basic setup uses a Hewlett-Packard 81101A pulse generator and a Tektronik TDS5034B DSO as described in [10] and [9]. Since neither commercial voltage sources nor pulse generators are able to fulfill the required settling specification of better than 10^{-4} in I_{D} within $< 1\,\mu\mathrm{s}$, a battery using a passive voltage divider and a fast electronic switch are used.

IV. Combined Stress and Relaxation Pulse Settings

Rectangular gate pulses were used for short-term NBTI stresses in the range of $1\,\mu\mathrm{s}$ to $1\,\mathrm{s}$, each followed by a full recovery sequence

978-1-4244-4353-6/09/$25.00 ©2009 IEEE

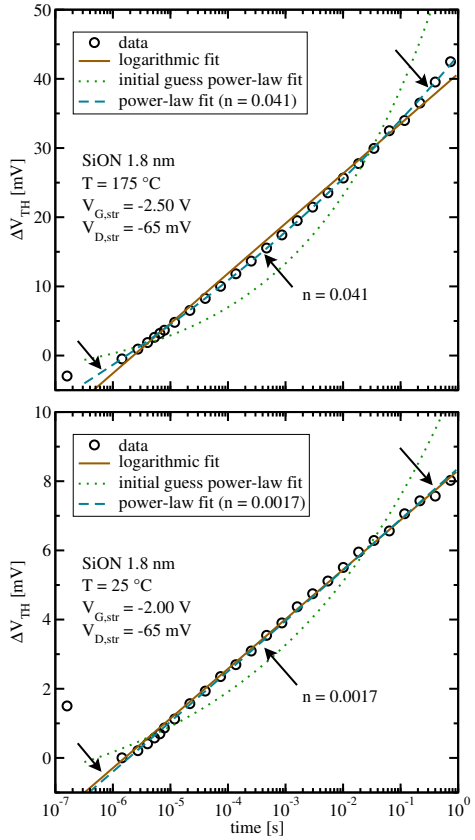

Fig. 1: **Top**: At the highest stress condition ($V_{\mathrm{G,str}} = -2.50\,\mathrm{V}$, $T = 175\,^{\circ}\mathrm{C}$) the recorded data slightly deviates from a logarithmic dependence and can be nicely fitted using a power-law. **Bottom**: By contrast, data recorded using a lower stress condition ($V_{\mathrm{G,str}} = -2.00\,\mathrm{V}$, $T = 25\,^{\circ}\mathrm{C}$) nearly perfectly follows a logarithmic behavior and cannot be properly fitted using a power-law.

Sequence	$t_{\mathrm{W}} = t_{\mathrm{str}}$	t_{rel}	t_{P}	N	Resolution
1	1 ms	99 ms	0.1 s	1000	0.16 μs
2	100 ms	9.9 s	10 s	10	16 μs
3	1000 ms	99 s	100 s	5	160 μs

TABLE I: Details of the rectangular stress pulses used to maximize the amount of recorded information together with the resolution.

being 100 times longer than the stress sequence itself [20]. Since a DSO can record data only on a linear time-scale but our experiments ask for a logarithmic time-scale spanning at least 6 decades, we split the total stress time of 1 s into three sub-intervals, and conduct separate stress/relaxation experiments for each sub-interval. This allows higher time resolution at the beginning of the stress phase and lower resolution at its end. Since the measurement noise decays with the inverse of the time resolution, with the slower sequences a lower averaging number is necessary to achieve a given amplitude resolution. Details of the pulse width $t_{\mathrm{W}} = t_{\mathrm{str}}$, the relaxation time t_{rel}, the pulse period t_{P}, and the number N of pulses per stress sequence are shown in Table I.

V. Data Extraction

The recorded degradation of the drain current is converted to an approximate threshold voltage shift using the simple OTF relation [11, 21]

$$\Delta V_{\mathrm{TH}}(t_{\mathrm{str}}/t_{0,\mathrm{ref}}) \approx \frac{\Delta I_{\mathrm{D}}(t_{\mathrm{str}})}{I_{\mathrm{D0}}}\,(V_{\mathrm{G}} - V_{\mathrm{TH}}) \qquad (1)$$

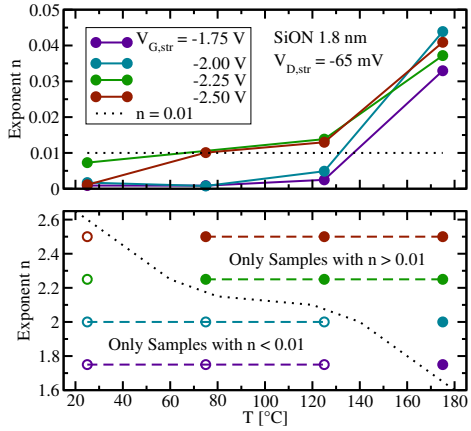

Fig. 2: **Top**: Only data recorded during heavier stress yield a reasonable power-law exponent n. **Bottom**: Using the (arbitrary) value of $n = 0.01$ as a threshold criterion, a high-stress region, where a deviation from the logarithmic behavior is observed, can be clearly identified.

with $\Delta I_{\mathrm{D}}(t_{\mathrm{str}}) = I_{\mathrm{D}}(t_{\mathrm{str}}) - I_{\mathrm{D0}}$ and $I_{\mathrm{D0}} = I_{\mathrm{D}}(t_{0,\mathrm{ref}})$. Note that I_{D0} is obtained at stress-level with a delay $t_{0,\mathrm{ref}}$ and is thus *not* equal to $I_{\mathrm{D}}(0)$ [22] resulting in an offset of the relative degradation. Also, the conversion (1) ignores any potential degradation in the mobility and is thus affected by an as-of-yet unknown error [13, 14]. V_{TH} is extracted at $I_{\mathrm{D}} = 70\,\mathrm{nA} * W/L$ and about $-0.3\,\mathrm{V}$. Then ΔV_{TH} is fitted by

$$\Delta V_{\mathrm{TH}}(t_{\mathrm{str}}/t_{0,\mathrm{ref}}) \approx B \log_{10}(t_{\mathrm{str}}/t_{0,\mathrm{ref}}) + C. \qquad (2)$$

In order to circumvent issues with the logarithmic fit caused by offset data due to the uncertainty in I_{D0}, the parameter C is included. Besides, it is tried to fit the data to a power-law of the form

$$\Delta V_{\mathrm{TH}}(t_{\mathrm{str}}/t_{0,\mathrm{ref}}) \approx A\,(t_{\mathrm{str}}/t_{0,\mathrm{ref}})^{n} + D. \qquad (3)$$

Again, the parameter D is introduced to account for the offset in I_{D0}.

Interestingly, it turns out that the logarithmic fit (2) is always possible while the power-law fit (3) produces reasonable results for high temperatures and high $V_{\mathrm{G,str}}$ only. In that high-stress regime, power-law exponents around 0.04 are obtained. For weaker stresses, the exponent n in (3) is reduced to zero by the optimizer, which corresponds to a first-order Taylor expansion of (3) on a logarithmic scale. As such, in this regime the power-law fit (3) becomes equivalent to the logarithmic fit (2).

This behavior is illustrated in Fig. 1. The data obtained from the harshest stress conditions ($V_{\mathrm{G,str}} = 2.50\,\mathrm{V}$, $T = 175\,^{\circ}\mathrm{C}$, and $t_{\mathrm{ox}} = 1.8\,\mathrm{nm}$) gives a stable fit with $n = 0.041$. For the other extreme case ($V_{\mathrm{G,str}} = 1.75\,\mathrm{V}$, $T = 25\,^{\circ}\mathrm{C}$, and $t_{\mathrm{ox}} = 1.8\,\mathrm{nm}$) the fit algorithm gives an exponent n of practically zero. For the case of the non-converging exponent n the logarithmic and power-law fits coincide.

Consequently, the power-law fit only makes sense for high temperatures and/or high $V_{\mathrm{G,str}}$, as displayed in Fig. 2. There, the extracted $n \approx 0.04$ for short-term stress is roughly one third of the often reported $n \approx 0.12$ of the long-term behavior.

VI. Settling Time Correction

In this section we are going to demonstrate that, in general, fast NBTI measurements have to be taken with a grain of salt. This, apart from other reasons not dealt with in this paper, is largely due to difficulties with synchronization between the stimulus

and the actual measurement. Even when the experiment is free of *systematic* synchronization errors, i.e. switching of the gate voltage and recording of I_D start at the same time, the finite settling time of real signals makes ex-post time zero adjustments necessary.

Fig. 3 displays V_G as a function of time during the stress phase and during the start of the relaxation phase. Reference values $V_\mathrm{G,str}^\mathrm{ref} = V_\mathrm{G}(t_\mathrm{str}/2)$ and $V_\mathrm{G,rel}^\mathrm{ref} = V_\mathrm{G}(2t_\mathrm{str})$ are determined, which represent the actual steady state values of $V_\mathrm{G,str}$ and $V_\mathrm{G,rel}$. Based on $V_\mathrm{G,str}^\mathrm{ref}$, the actual stress phase is defined as all consecutive points extending to both sides of the point $t = t_\mathrm{str}/2$ that fulfill the criterion $|(V_\mathrm{G} - V_\mathrm{G,str}^\mathrm{ref})/V_\mathrm{G,str}^\mathrm{ref}| \leq \epsilon$; usually $\epsilon \approx 0.3\,\%$.

Handling of the relaxation phase is trickier. Arguing that the noise level is the same during stress and relaxation (the DSO continuously records, using the same settings), and the settling time of the pulse generator in theory is equal regardless if switching from $V_\mathrm{G,rel}$ to $V_\mathrm{G,str}$ or vice versa occurred, the criterion for the relaxation phase could be established as 'all points extending to both sides of $t = 2t_\mathrm{str}$ that fulfill $|(V_\mathrm{G} - V_\mathrm{G,rel}^\mathrm{ref})/V_\mathrm{G,str}^\mathrm{ref}| \leq \epsilon$'. This effectively uses the same *absolute* allowed deviation from $V_\mathrm{G,rel}^\mathrm{ref}$ as was used during determination of the stress phase, hence this method will be referred to as the 'ϵ_abs-criterion'. On the other hand, the relative error in I_D (and hence in ΔV_TH) that would erroneously be attributed to NBTI is given by the *relative* deviation of V_G, asking for a criterion $|(V_\mathrm{G} - V_\mathrm{G,rel}^\mathrm{ref})/V_\mathrm{G,rel}^\mathrm{ref}| \leq \epsilon$. This method, which is tighter by a factor of $|V_\mathrm{G,str}/V_\mathrm{G,rel}| \approx 7$, is referred to as the 'ϵ_rel-criterion'. Both methods were investigated thoroughly, and the relative method was chosen.

For relaxation, based on the assumption of full recovery after each stress/relaxation cycle, $I_\mathrm{D0,rel} = I_\mathrm{D}(t_\mathrm{P})$ is chosen, implying $\Delta I_\mathrm{D}(t_\mathrm{P}) = 0$. Therefore $I_\mathrm{D0,rel}$ is independent of ϵ, whereas $I_\mathrm{D0,str} = I_\mathrm{D}(t_\mathrm{0,ref})$ depends on the ϵ used. Note that due to record length constraints of the DSO, not the entire relaxation characteristic up to t_P is recorded, but only the initial relaxation up to around three to four times t_str. The point $t = t_\mathrm{P}$ nevertheless is available in the pre-trigger data of the DSO.

Data extraction turns out to be extremely sensitive to the choice of ϵ, indicating that the settling time of V_G plays a crucial role in OTF experiments. To demonstrate this fact, the top of Fig. 4 shows relaxation after $t_\mathrm{str} = 1\,\mathrm{ms}$ for different values of ϵ. If the criterion is too conservative, i.e. ϵ is chosen small, thereby cutting off the initial relaxation phase, the shape of the relaxation characteristics is significantly altered. On the other hand, too large values of ϵ, i.e. too liberal limits for gate voltage settling, may produce spurious relaxation transients. Assuming the relaxation follows $\log(t_\mathrm{rel}/t_0)$ as indicated by the red curve in Fig. 4, setting the starting point of the extracted relaxation to later times (through smaller ϵ) gives a dependence of $\log((t_\mathrm{rel} + \Delta t)/t_0)$, which produces the artificial plateaus seen with the blue curves in the figure. Possibly the saturation towards smaller relaxation times found in [6, 23, 24] can be explained in this way, i.e. the plateaus observed are not a feature of NBTI relaxation but an artifact due to finite settling times and synchronization inaccuracies, in turn invalidating the assertion that a measurement delay in the micro-second regime is sufficient to correctly capture the relaxation characteristics of NBTI.

VII. Comparison of Relaxation using the On-The-Fly-method and the Fast-V_TH-method

For $t_\mathrm{str} = 1\,\mathrm{ms}$ a comparison of different voltages and temperatures is examined in the following, cf. the bottom of Fig. 4.

Taking into account that the temperature dependence of V_TH0 was not exactly measured, and hence is missing for the precise ΔV_TH extraction and additionally neglecting mobility changes with temperature still show well qualitative conformity with the relaxation curves of the Fast-V_TH measurement.

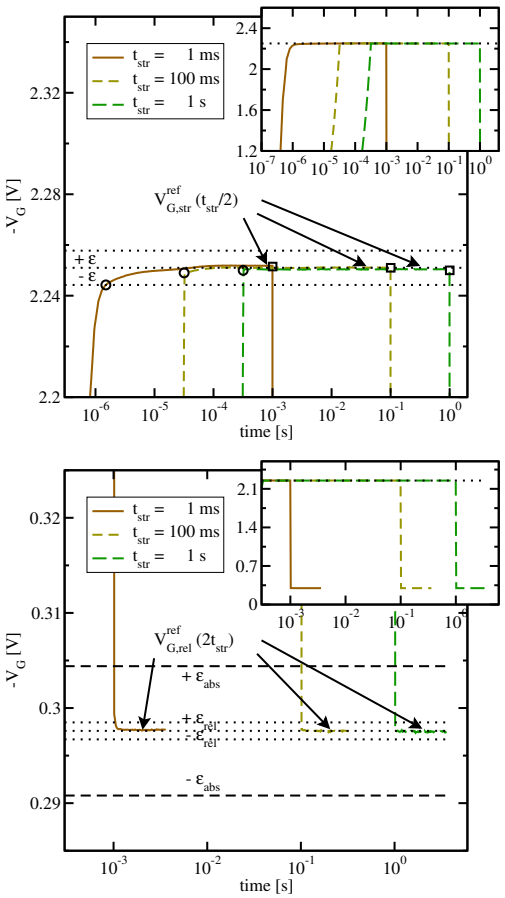

Fig. 3: **Top**: The main graph is enlarged to make the transient and the overshoot visible. The bounds due to the error criterion $|(V_\mathrm{G} - V_\mathrm{G,str}^\mathrm{ref})/V_\mathrm{G,str}^\mathrm{ref}| \leq \epsilon$ are displayed for $\epsilon = 0.3\,\%$. The first (last) proper values of the pulse for each sequence are marked by circles (squares). **Bottom**: The bounds for both the relative and the absolute criterion are depicted.

VIII. Conclusions

Fast down to 1 μs-methods are unavoidable when extracting ΔI_D or ΔV_TH properly to better understand NBTI-stress and relaxation. The initial NBTI degradation is often explained by elastic hole trapping which also considerably distorts long-term measurements. In this initial degradation phase, the data can be well fit by a logarithmic time dependence [9, 10, 15, 23], being rather stable compared to the frequently reported power-law using an exponent n remarkably smaller ($n \approx 0.04$) than generally observed during long-time stress ($n \approx 0.12$). The main disadvantage of the power-law is that the fit is ill defined for up to medium stress conditions. Only high temperatures and/or high $V_\mathrm{G,str}$ show the aforementioned small n. The investigated short-time behavior of **stress and relaxation** accounts for a thermally activated tunneling mechanism and clearly rules out elastic and thus temperature-independent hole tunneling. Moreover, the comparison to the completely different fast-V_TH measurement routine revealed new interesting results concerning the time constants of the relaxation sequence. It seems that too early cutting off the data in addition to a limited resolution of smaller than 1 μs leads to an artificially created

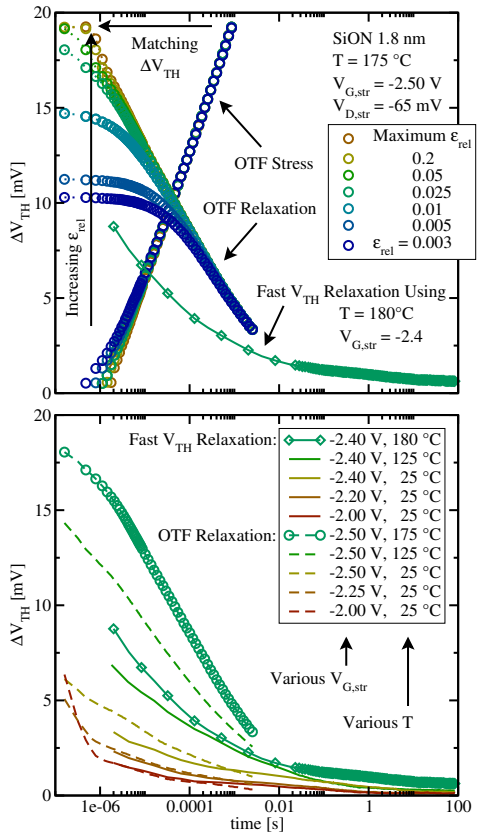

Fig. 4: Comparison of the fast-V_{TH} measurement and our on-the-fly-method. **Top**: Depending on the relative epsilon criterion ϵ_{rel}, more or less points are considered for the relaxation curves leading to different initial slopes. While $\epsilon_{\mathrm{rel}} = 0.003$ results in an artifact, as the data points are stretched out towards shorter times, $\epsilon_{\mathrm{rel}} = 0.025$ shows good agreement with the data gained from the fast-V_{TH} measurement, which does not have a plateau. **Bottom**: As not exactly the same parameter set was available for the two different measurement setups matchable curves are plotted in the same colors and show quite good conformity.

plateau indicating wrong time constants of the involved mechanisms if the remaining data is not evaluated with extreme caution.

Acknowledgment

The research leading to these results has received funding from the European Community's Seventh Framework Programme under grant agreement n°216436 (project ATHENIS).

References

[1] V. Huard, M. Denais, and C. Parthasarathy, "NBTI Degradation: From Physical Mechanisms to Modelling," *Microelectronics Reliability*, vol. 46, no. 1, pp. 1–23, 2006.

[2] D.K. Schroder and J.A. Babcock, "Negative Bias Temperature Instability: Road to Cross in Deep Submicron Silicon Semiconductor Manufacturing," *J. Appl. Phys.*, vol. 94, no. 1, pp. 1–18, Jul. 2003.

[3] H. Reisinger, O. Blank, W. Heinrigs, A. Mühlhoff, W. Gustin, and C. Schlünder, "Analysis of NBTI Degradation- and Recovery-Behavior Based on Ultra Fast V_{TH}-Measurements," in *Proc. Intl.Rel.Phys.Symp.*, 2006, pp. 448–453.

[4] M. Denais, V. Huard, C. Parthasarathy, G. Ribes, F. Perrier, N. Revil, and A. Bravaix, "Interface Trap Generation and Hole Trapping under NBTI and PBTI in Advanced CMOS Technology with a 2-nm Gate Oxide," *T-DMR*, vol. 4, pp. 715–722, 2004.

[5] S. Mahapatra, V.D. Maheta, A.E. Islam, and M.A. Alam, "Isolation of NBTI Stress Generated Interface Trap and Hole-Trapping Components in PNO p-MOSFETs," *T-ED*, vol. 56, no. 2, pp. 236–242, Feb. 2009.

[6] V.D. Maheta, E.N. Kumar, S. Purawat, C. Olsen, K. Ahmed, and S. Mahapatra, "Development of an Ultrafast On-the-Fly I_{DLIN} Technique to Study NBTI in Plasma and Thermal Oxynitride p-MOSFETs," *T-ED*, vol. 55, no. 10, pp. 2614–2622, Oct. 2008.

[7] T. Grasser and B. Kaczer, "Evidence that Two Tightly Coupled Mechanisms are Responsible for Negative Bias Temperature Instability in Oxynitride MOSFETs," *T-ED*, 2009, (in print).

[8] T. Grasser, B. Kaczer, W. Gös, Th. Aichinger, Ph. Hehenberger, and M. Nelhiebel, "A Two-Stage Model for Negative Bias Temperature Instability," in *IRPS*, 2009.

[9] Ph. Hehenberger, P.-J. Wagner, H. Reisinger, and T. Grasser, "On the Temperature and Voltage Dependence of Short-Term Negative Bias Temperature Stress," in *ESREF*, 2009, submitted.

[10] H. Reisinger, U. Brunner, W. Heinrigs, W. Gustin, and C. Schlünder, "A Comparison of Fast Methods for Measuring NBTI Degradation," *T-DMR*, vol. 7, no. 4, pp. 531–539, Dec. 2007.

[11] A.T. Krishnan, V. Reddy, S. Chakravarthi, J. Rodriguez, S. John, and S. Krishnan, "NBTI Impact on Transistor & Circuit: Models, Mechanisms & Scaling Effects," in *IEDM*, 2003, pp. 1–4.

[12] M. Denais, A. Bravaix, V. Huard, C. Parthasarathy, G. Ribes, F. Perrier, Y. Rey-Tauriac, and N.Revil, "On-the-Fly Characterization of NBTI in Ultra-Thin Gate Oxide PMOSFETs," in *IEDM*, 2004.

[13] T. Grasser, P.-J. Wagner, Ph. Hehenberger, W. Gös, and B. Kaczer, "A Rigorous Study of Measurement Techniques for Negative Bias Temperature Instability," *T-DMR*, vol. 8, no. 3, pp. 526–535, Sep. 2008.

[14] A.E. Islam, E.N. Kumar, H. Das, S. Purawat, V. Maheta, H. Aono, E. Murakami, S. Mahapatra, and M.A. Alam, "Theory and Practice of On-The-Fly and Ultra-Fast VT Measurements for NBTI Degradation: Challenges and Opportunities," in *IEDM*, 2007, pp. 805–808.

[15] H. Reisinger, O. Blank, W. Heinrigs, W. Gustin, and C. Schlünder, "A Comparison of Very Fast to Very Slow Components in Degradation and Recovery due to NBTI and Bulk Hole Trapping to Existing Physical Models," *T-DMR*, vol. 7, no. 1, pp. 119–129, Mar. 2007.

[16] B. Kaczer, T. Grasser, Ph.J. Roussel, J. Martin-Martinez, R. O'Connor, B.J. O'Sullivan, and G. Groeseneken, "Ubiquitous Relaxation in BTI Stressing New Evaluation and Insights," in *IRPS*, 2008.

[17] B. Kaczer, V. Arkhipov, R. Degraeve, N. Collaert, G. Groeseneken, and M. Goodwin, "Disorder-Controlled-Kinetics Model for Negative Bias Temperature Instability and its Experimental Verification," in *IRPS*, 2005, pp. 381–387.

[18] T. Grasser, B. Kaczer, P. Hehenberger, W. Gös, R. O'Connor, H. Reisinger, W. Gustin, and C. Schlünder, "Simultaneous Extraction of Recoverable and Permanent Components Contributing to Bias-Temperature Instability," in *IEDM*, 2007.

[19] C. Shen, M.-F. Li, X.P. Wang, Y.-C. Yeo, and D.-L. Kwong, "A Fast Measurement Technique of MOSFET Id-Vg Characteristics," *EDL*, vol. 27, no. 1, pp. 55–57, 2006.

[20] S. Rangan, N. Mielke, and E.C.C. Yeh, "Universal Recovery Behavior of Negative Bias Temperature Instability," in *IEDM*, 2003, pp. 341–344.

[21] S. Mahapatra, K. Ahmed, D. Varghese, A. E. Islam, G. Gupta, L. Madhav, D. Saha, and M. A. Alam, "On the Physical Mechanism of NBTI in Silicon Oxynitride p-MOSFETs: Can Differences in Insulator Processing Conditions Resolve the Interface Trap Generation versus Hole Trapping Controversy?," in *Proc. Intl.Rel.Phys.Symp.*, 2007, pp. 1–9.

[22] C. Shen, M.-F. Li, C.E. Foo, T. Yang, D.M. Huang, A. Yap, G.S. Samudra, and Y.-C. Yeo, "Characterization and Physical Origin of Fast Vth Transient in NBTI of pMOSFETs with SiON Dielectric," in *IEDM*, 2006.

[23] J.F. Zhang, Z. Ji, M.H. Chang, B. Kaczer, and G. Groeseneken, "Real Vth Instability of pMOSFETs under Practical Operation Conditions," in *IEDM*, 2007, pp. 817–820.

[24] E.N. Kumar, V.D. Maheta, S. Purawat, A.E. Islam, C. Olsen, K. Ahmed, M.A. Alam, and S. Mahapatra, "Material Dependence of NBTI Physical Mechanism in Silicon Oxynitride (SiON) pMOSFETs: A Comprehensive Study by Ultra-Fast On-The-Fly (UF-OTF) I_{DLIN} Technique," in *IEDM*, 2007, pp. 809–812.